Space distribution of preshocks

G.F. Karakaisis, C.B. Papazachos, D.G. Panagiotopoulos, E.M. Scordilis and B.C. Papazachos

Department of Geophysics, School of Geology, Thessaloniki, Greece

(Received: December 5, 2006; accepted: June 20, 2007)

ABSTRACT The space distribution of decelerating and accelerating preshocks is examined for six samples of forty-three mainshocks which have occurred recently in the western Mediterranean, the Aegean Sea, Anatolia, California, Japan and central Asia. It is observed that the frequency of shocks of a decelerating or accelerating preshock seismic sequence decays rapidly with distance from an easily located distinct geographical point according to a power-law. This point is defined as the physical center of the decelerating P_f, and the accelerating P_q, preshocks, respectively. On the basis of the mean distance and the corresponding uncertainty of the forty-three mainshock epicenters taken from the corresponding physical centers of the decelerating and accelerating preshocks, respectively, a simple procedure is proposed for a possible contribution of the locations of the two physical centers of preshocks to the location of an ensuing mainshock.

Introduction

Foreshocks (in the classical sense) are generated shortly (days to weeks) before the mainshock and within its rupture zone. The number and magnitudes of foreshocks are usually small and for this reason they cannot be easily distinguished from background seismic activity before the generation of the mainshock. However, research work during the last four decades has shown that there are other shocks which also precede mainshocks but are larger than foreshocks, and occur over a much longer time period (years to decades) and in a much broader region. These are called "preshocks" and several of their properties indicate that they are physically related to the ensuing mainshock. There are "accelerating preshocks" and "decelerating preshocks" of a mainshock that occur in different space, time and magnitude windows.

Accelerating intermediate magnitude preshocks have been observed before many strong mainshocks by several workers (Tocher, 1959; Sykes and Jaumé, 1990; Knopoff *et al*., 1996; Brehm and Braile, 1999; Robinson, 2000; Tzanis *et al*., 2000; Papazachos and Papazachos, 2001, among many others). Attempts have been made to interpret accelerating preshock sequences in terms of the critical point dynamics (Sornette and Sornette, 1990; Allègre and Le Mouël, 1994; Sornette and Sammis, 1995; Rundle *et al*., 2000, 2003). Bufe and Varnes (1993) proposed the following relation for the time variation of the cumulative Benioff strain (sum of the square root of seismic energy), $S(t)$, released by the accelerating preshocks:

$$S(t) = A + B\left(t_c - t\right)^m \tag{1}$$

where t_c is the origin time of the mainshock, t is the time to the mainshock and A, B, m, are parameters determined by observations, with $m<1$. It has been shown (Papazachos *et al*., 2005a, 2006a) that the circular region, where accelerating preshocks occur (critical region), has its center, $Q(\varphi,\lambda)$, at some distance from the mainshock epicenter. The radius, R, of this region increases with the mainshock magnitude M (Bowman *et al*., 1998; Papazachos and Papazachos, 2000, 2001), decreases with the long-term strain rate, s_a (in Joule$^{1/2}$/yr·10^{4}km^2), and is about eight times the fault length of the mainshock. The duration of an accelerating preshock sequence also decreases with the long-term strain rate, s_a (Papazachos *et al*., 2005a, 2006a). The minimum magnitude, M_{min}, of an accelerating preshock sequence is given by the relation:

$$M_{\min} = 0.46M + 1.91. \quad (2)$$

Thus for mainshock magnitude 6.0 the minimum magnitude of accelerating preshocks is 4.7.

Transient seismic excitation near the fault region, which is followed by a continuous decrease of seismic activity, has been called "decelerating seismicity" and was also shown to follow Eq. (1) but with $m>1$ (Papazachos *et al*., 2005b). It has been further shown (Papazachos *et al*., 2006a) that the region where decelerating preshocks of a mainshock occur (seismogenic region) can be assumed to be circular with a center, $F(\varphi,\lambda)$, which does not coincide with the epicenter of the mainshock. The radius, R_d, of this region increases with the mainshock magnitude M, decreases with the long-term seismicity rate, s_d (in Joule$^{1/2}$/yr·10^{4}km^2), and is about four times the fault length of the mainshock. The duration, t_c-t_{sd}, of a decelerating preshock sequence scales also negatively with s_d (t_{sd} is the start time of the decelerating sequence). The minimum magnitude, M_{min}, of a decelerating preshock sequence is given by the relation:

$$M_{\min} = 0.29M + 2.35 \quad (3)$$

where M is the mainshock magnitude. Thus for mainshock magnitude 6.0 the smallest decelerating preshock has a value equal to 4.1.

The goal of the present work is to use data concerning preshocks of recently occurred strong mainshocks in the western Mediterranean, the Aegean Sea, Anatolia, California, Japan and central Asia to study the distribution of the epicentres of these preshocks and to show how this distribution can probably contribute to the estimation (prediction) of the epicenter of an ensuing mainshock.

Karakaisis *et al*. (2007) used global data to examine the frequency-magnitude variation with the time to the mainshock for accelerating and decelerating preshock sequences. They observed that the ratio, a/b, of the parameters in the Gutenberg-Richter relation varies with time. This ratio increases with time for accelerating sequences, which means a corresponding increase of the magnitude of accelerating preshocks with the time to the mainshock. They also observed that for the decelerating preshock sequences this ratio initially decreases with time and during the last 40% of the duration of these sequences increases slightly, which indicates a corresponding change of the magnitude of the decelerating preshocks.

Eq. (1) is a power-law which for decelerating preshocks ($m>1$) is similar to the revised

Omori's law that holds for aftershocks of a mainshock, since these aftershocks also comprise a decelerating sequence. Eq. (1) with $m<1$ is also similar to the inverse of revised Omori's law which holds for some foreshock sequences. However, it must be noted that Eq. (1) describes the time variation of the Benioff strain which is dominated by intermediate magnitude preshocks, whereas revised Omori's law (or its inverse) describes the time variation of the frequency (number per unit time) of aftershocks (or foreshocks), which is dominated by the small magnitude shocks.

2. Data

The data used in the present work concern parameters of decelerating and accelerating preshock sequences of strong mainshocks that occurred recently (since 1980) in the western Mediterranean, the Aegean Sea, Anatolia, California, Japan and central Asia. For the western Mediterranean, the Aegean Sea, Anatolia and California, preshock sequences of all mainshocks that occurred there between 1980 and 2004 and had moment magnitudes $M\geq 6.4$ were considered. For Japan and central Asia, preshock sequences of all mainshocks that occurred between 1990 and 2005 but with $M\geq 7.0$ were considered due to the fact that most of the shocks with $M<7.0$ are associated earthquakes (preshocks, aftershocks) there. Eighteen such mainshocks occurred in the Mediterranean (four in the western Mediterranean, nine in the Aegean, five in Anatolia), eight in California, eight in Japan and nine in central Asia. The origin times, t_c, epicenter coordinates, $E(\varphi,\lambda)$, and magnitudes, M, for these forty-three mainshocks are listed in Table 1.

The identification of the circular regions where decelerating preshock seismicity occurred (seismogenic regions), the circular regions where accelerating preshock seismicity occurred (critical regions) and the parameters of the corresponding preshocks has been made by Papazachos *et al*. (2006a). The values of these parameters are given in Table 1. $F(\varphi,\lambda)$ and R_d are the center and the radius of the seismogenic region, M_{min} is the minimum magnitude of the decelerating preshocks, n is the number and t_{sd} is the start time of these preshocks. Similarly $Q(\varphi,\lambda)$ and R_a are the center and the radius of the critical region, and M_{min}, n, t_{sa} are the minimum magnitude, the number and the start time of the accelerating preshocks. Parameters for all these shocks are listed in catalogues published by Papazachos *et al*. (2006b) for the Mediterranean, by Karakaisis *et al*. (2006) for California and by Scordilis *et al*. (2006a, 2006b) for Japan and central Asia.

3. Procedure followed to compile the earthquake catalogue for each preshock sequence

To study the space distribution of the density of the epicenters of preshocks, it is necessary to compile a catalogue for each decelerating preshock sequence, as well as for each accelerating preshock sequence. The catalogue must include the magnitude, the date and the epicenter coordinates of each preshock of the sequence. This is done on the basis of the magnitude, time and space windows defined by Papazachos *et al*. (2006a) for each of the eighty-six preshock sequences (43 decelerating and 43 accelerating sequences).

The minimum magnitude for the shocks of a preshock sequence depends on the magnitude of the mainshock and is given by the Eq. (2) for the accelerating sequences and by the Eq. (3) for

the decelerating sequences. The constraint imposed on the magnitude of the largest preshock is that this is smaller than the mainshock magnitude (usually M-M_{max}<0.4).

The time window of a preshock sequence depends on the seismicity level, s (in Joule$^{1/2}$/yr·10^{4}km^2), of the region. The end of this window depends on the origin time of the mainshock and the start time is given by the relation (5) in Papazachos *et al*. (2006a) for accelerating preshock sequences and by the relation (9) in Papazachos *et al*. (2006a) for decelerating preshock sequences.

The radius of the circular region where preshocks occur depends on the mainshock magnitude and on the seismicity level of the region and is given by the relation (3) in Papazachos *et al*. (2006a) for accelerating preshocks (critical region) and by the relation (8) in Papazachos *et al*. (2006a) for decelerating preshocks (seismogenic region). The center, Q, of the circular critical region and the center, F, of the circular seismogenic region are defined by an optimization procedure (Papazachos *et al*., 2006a). This optimization procedure is based on minimization of a curvature parameter, C, defined by Bowman *et al*. (1998) as the ratio of the root-mean-square error of the power-law fit [Eq. (1)] to the corresponding linear fit error. That is, the values of C are calculated for each point of a grid and the point where C takes its smallest value is the center, Q, of the critical region when data of accelerating preshocks are used and the center, F, of the seismogenic region when data of decelerating preshocks are used.

Thus, to know of the magnitude range, of the time interval and of the circular area of location of all shocks of a preshock sequence allows the compilation of a catalogue of shocks for each preshock sequence, which can be used for the investigation of the space variation of the epicenters of preshocks. The decelerating preshock sequence of a mainshock occurs in partly different space, time and magnitude windows with respect to the accelerating sequence of the same mainshock, as it comes out from the relations which define these windows. For example, for the big (M=8.3) mainshock that occurred on 4.10.1994 in northern Japan, the magnitude of the smallest accelerating preshock is 5.7 [Eq. (2)] and of the smallest decelerating preshock is 4.8 [Eq. (3)] . For the same mainshock the radius of the circular and seismogenic region is 782 km and 291 km, respectively, and the start times of the two sequences are also different (see Fig. 1). It has to be mentioned that the preshock seismic excitation in a broad region and the seismic quiescence in the narrower focal region of an oncoming mainshock has been called “doughnut pattern” by Mogi (1969).

4. Variation of the frequency of preshocks with distance

To investigate the space distribution of decelerating and accelerating preshocks, the variation of the frequency (number per unit area) of their epicentres with the distance from several geographic points of a broad region (e.g. with dimensions 400 km by 400 km and grid density 0.2°N-S, 0.2°E-W) was examined for each decelerating and each accelerating preshock sequence. A systematic rapid decrease with the distance of the frequency of decelerating preshocks from a distinct geographic point, P_f, was observed for each one of the forty-three decelerating preshock sequences. The same behaviour was observed for each accelerating preshock sequence, that is, a decrease of the frequency from another point, P_q.

To further examine this behaviour, we have assumed that the spatial density of preshocks,

Table 1 - Information on the data used in the present work. t_c, E, M are the origin time, epicentre and magnitude of the forty-three mainshocks. F and Q are the centers of the circular regions where the epicentres of the decelerating and accelerating preshocks, respectively, are located. R is radius of the corresponding region, M_{min} is the minimum preshock magnitude, n is the number of preshocks and t_s is the start year of the corresponding sequence.

t_c	E(φ,λ)	M	F(φ,λ)	M_{min}	R_d	t_{sd}	n_d	Q(φ,λ)	M_{min}	R_a	t_{sa}	n_a
W.Medit.												
1. 1980.10.10	36.2, 01.4	7.1	35.7, 02.4	4.3	272	1955	84	36.2, 00.6	5.1	277	1912	21
2. 1980.11.23	40.8, 15.3	6.9	42.0, 14.3	4.3	178	1960	142	44.0, 13.8	5.2	338	1945	53
3. 2003.05.21	36.9, 03.8	6.8	34.9, 04.2	4.4	220	1961	46	38.6, 06.0	5.2	770	1924	96
4. 2004.02.24	35.1, -04.0	6.4	36.3, -05.8	4.1	175	1966	37	33.8, -01.8	4.6	198	1919	21
Aegean												
1. 1980.07.09	39.3, 22.9	6.5	39.6, 21.9	4.2	98	1969	61	37.8, 24.1	4.6	137	1954	37
2. 1981.02.24	38.1, 23.0	6.7	38.1, 24.0	4.4	133	1964	126	36.8, 21.7	5.1	263	1967	45
3. 1981.12.19	39.0, 25.3	7.2	38.0, 27.3	4.5	172	1964	156	37.0, 23.1	5.1	277	1967	47
4. 1983.01.17	38.1, 20.2	7.0	38.5, 19.5	4.5	105	1970	103	37.4, 18.7	4.9	237	1963	32
5. 1995.05.13	40.2, 21.7	6.6	39.3, 21.4	4.4	138	1981	236	41.2, 21.4	5.0	168	1973	21
6. 1997.10.13	36.4, 22.2	6.4	36.4, 23.0	4.3	117	1984	58	37.0, 22.2	4.8	138	1970	81
7. 1997.11.18	37.5, 20.7	6.6	37.0, 21.6	4.3	140	1981	570	39.6, 21.6	5.0	181	1985	27
8. 2001.07.26	39.1, 24.4	6.4	38.3, 24.1	4.2	113	1987	80	37.6, 26.4	5.0	163	1980	34
9. 2003.08.14	38.7, 20.5	6.4	38.7, 21.0	4.2	95	1992	157	37.3, 19.0	4.7	137	1984	29
Anatolia												
1. 1983.07.05	40.2, 27.3	6.4	40.2, 28.1	4.3	119	1968	92	28.2, 26.0	4.7	142	1960	21
2. 1992.03.13	39.7, 39.6	6.6	38.7, 39.1	4.2	122	1975	26	37.7, 38.9	5.0	175	1912	21
3. 1995.10.01	38.1, 30.2	6.4	39.1, 30.2	4.2	131	1983	45	35.7, 28.2	4.8	226	1977	108
4. 1996.10.09	34.5, 32.1	6.8	35.0, 31.4	4.3	164	1977	24	34.3, 30.3	4.8	200	1930	34
5. 1999.08.17	40.8, 30.0	7.5	40.6, 31.5	4.5	230	1982	31	38.6, 29.5	5.1	310	1980	35
California												
1. 1980.11.08	41.1,-124.6	7.3	42.1,-124.1	4.4	136	1960	22	41.6,-125.6	5.1	249	1957	29
2. 1983.05.02	36.2,-120.3	6.4	35.0,-120.3	4.1	103	1964	22	38.0,-122.5	4.7	218	1931	65
3. 1987.11.24	33.0,-115.9	6.6	32.0,-116.9	4.3	159	1966	37	35.4,-118.3	5.0	283	1961	83
4. 1989.10.18	37.1,-121.9	6.9	36.3,-123.1	4.4	160	1967	25	37.6,-122.4	5.2	375	1943	93
5. 1992.04.25	40.3,-124.2	7.1	39.3,-123.2	4.4	201	1967	117	37.3,-123.2	5.1	431	1943	139
6. 1992.06.28	34.2,-116.4	7.3	35.8,-116.4	4.6	246	1969	108	33.5,-116.9	5.2	468	1953	86
7. 1994.01.17	34.2,-118.5	6.6	33.2,-119.5	4.1	144	1975	21	34.9,-119.0	4.8	186	1972	21
8. 2003.12.22	35.7,-121.1	6.5	35.7,-122.1	4.3	141	1982	23	33.7,-120.9	4.9	375	1956	76
Japan												
1. 1993.07.12	42.9, 139.2	7.7	41.5, 139.7	4.5	203	1984	200	45.3, 136.8	5.6	636	1955	46
2. 1994.10.04	43.7, 147.4	8.3	43.1, 146.6	4.8	291	1975	1629	41.7, 148.4	5.7	782	1982	158
3. 1995.01.16	34.6, 135.0	7.0	35.3, 135.0	4.5	142	1983	108	35.4, 133.2	5.1	693	1972	285
4. 2003.05.25	38.8, 141.6	7.0	39.1, 141.8	4.3	126	1996	360	38.1, 139.6	4.9	201	1989	70
5. 2003.09.25	41.8, 143.9	8.3	42.3, 143.4	4.8	199	1994	159	41.8, 143.4	5.8	1340	1984	273
6. 2003.10.31	37.8, 142.6	7.0	37.1, 143.6	4.3	127	1994	157	39.8, 141.1	5.0	180	1997	32
7. 2004.09.05	33.7, 137.1	7.4	33.2, 137.1	4.5	213	1990	201	31.7, 135.6	5.2	431	1985	107
8. 2005.08.16	38.3, 142.0	7.2	39.3, 141.2	4.3	140	1995	612	40.2, 141.2	5.0	185	1997	44
Central Asia												
1. 1990.06.20	37.0, 49.3	7.4	35.8, 48.5	4.5	233	1956	64	34.6, 51.6	5.7	910	1940	73
2. 1992.08.19	42.1, 73.6	7.2	43.1, 73.4	4.4	167	1968	21	42.2, 74.8	5.0	310	1959	54
3. 1997.02.27	30.0, 68.2	7.0	31.0, 68.5	4.2	108	1979	25	28.0, 70.2	5.2	526	1940	113
4. 1997.05.10	33.9, 59.8	7.3	35.4, 58.3	4.4	191	1974	64	30.7, 63.0	5.3	593	1941	99
5. 1997.11.08	35.1, 87.4	7.5	34.3, 86.9	4.4	238	1972	97	36.8, 87.5	5.4	630	1944	45
6. 2000.12.06	39.6, 54.8	7.0	41.1, 54.3	4.4	244	1982	83	39.6, 53.7	5.1	458	1958	68
7. 2001.01.26	23.4, 70.2	7.6	23.9, 66.8	4.6	284	1972	44	25.6, 67.8	5.2	510	1946	51
8. 2001.11.14	35.9, 90.5	7.8	37.1, 92.7	4.6	319	1985	44	37.4, 88.3	5.4	590	1940	43
9. 2005.10.08	34.5, 73.6	7.5	38.0, 73.7	4.5	265	1988	554	31.5, 74.1	5.3	604	1976	76

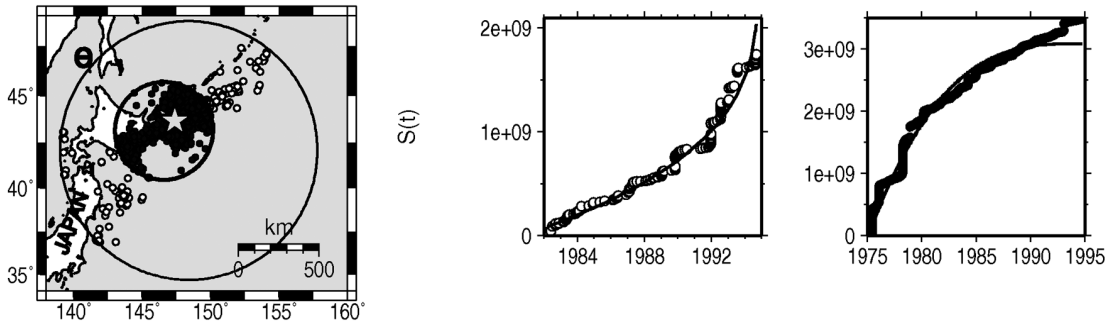

Fig. 1 - An example of the accelerating and decelerating seismic sequence that preceded the October 4, 1994, mainshock (M=8.3) in Japan [Fig. 2e in Papazachos *et al*. (2006a)]. The mainshock epicentre is denoted by the star. The epicentres of accelerating preshocks that occurred within the critical region (large circle) are denoted by small open circles whereas the epicentres of the decelerating preshocks, that occurred within the seismogenic region (small circle), are denoted by small solid circles. The time variation of the cumulative Benioff strain, $S(t)$, is also shown for the accelerating sequence (left plot) and decelerating sequence (right plot). Solid lines represent the fitting of a power-law [Eq. (1)] to the data.

dn/dS, follows a power-law:

$$\frac{dn}{dS} = \beta \cdot \Delta^d \tag{4}$$

where Δ is the distance from the geographic point, P, and β, d are appropriate constants. It is clear that if d=0, the spatial distribution of preshocks is constant (=β). Integrating Eq. (4) between Δ=0 and an arbitrary distance Δ gives (in a logarithmic form):

$$\log N = B + D \log \Delta \tag{5}$$

where N is the cumulative number of preshocks which have occurred up to distance Δ, D=d+2, B=log(2$\pi\beta$/D). It is clear that if D≈2, the spatial density of preshocks is practically constant, whereas D<<2 values suggest a strong spatial power-law decay of preshocks from point P. Eq. (5) has been used for the modeling of the spatial distribution of preshocks in the present work.

As distinct geographic point, P, of a preshock sequence, we consider the point for which D takes its smallest value from all values of a grid of points in the area under study. As the center of the studied area, the geometric center, F (±2°N-S, ±2°E-W), is used to define P_f for decelerating preshocks and P_q for accelerating preshocks.

Table 2 shows the geographic coordinates of points P_f and P_q, where D obtains its smallest value for the decelerating and accelerating preshock sequences, respectively. In the same table, the corresponding values, D_f, D_q, of the exponents of Eq. (5) are given. The average value for decelerating preshock sequences is D_f=0.66±0.23 while for accelerating preshock sequences the corresponding value is D_q=0.86±0.25. The linear correlation coefficient between log$N$ and logΔ

Table 2 - The physical centers of the seismogenic region, P_f, and of the critical region, P_q, from which the frequency of the decelerating preshocks and accelerating preshocks, respectively, decay with increasing distance according to a power-law [Eq. (5)]. D_f and D_q are the corresponding exponents of this relation for each preshock sequence.

	P_f	D_f	P_q	D_q
W. Medit.				
1	36.3, 01.6	0.52	36.3, 01.4	0.49
2	42.8, 13.1	0.39	41.6, 15.9	0.81
3	36.5, 04.2	0.86	35.5, 03.0	0.83
4	36.3, -07.6	0.82	35.5, -03.2	1.05
Aegean				
1	39.0, 21.5	0.75	38.0, 22.9	0.74
2	39.1, 24.0	0.66	38.1, 22.6	0.86
3	39.3, 23.1	0.55	38.6, 22.7	0.72
4	37.9, 20.1	0.51	37.9, 20.3	0.55
5	38.5, 20.6	0.79	40.9, 20.2	0.71
6	36.0, 22.0	0.86	37.6, 21.2	0.82
7	37.8, 20.8	0.65	38.2, 22.2	0.76
8	39.1, 23.5	0.83	38.7, 25.3	0.64
9	38.1, 20.4	0.97	37.7, 20.2	0.66
Anatolia				
1	37.9, 28.3	0.70	38.4, 27.3	0.95
2	37.9, 38.5	0.74	38.1, 38.5	0.78
3	39.1, 29.0	0.58	37.1, 29.2	0.86
4	34.8, 32.4	0.69	35.6, 30.8	0.83
5	40.6, 29.5	0.34	40.6, 29.5	1.40
California				
1	42.1, -125.5	0.74	40.1, -124.7	0.78
2	34.2, -119.9	0.33	37.0, -121.5	0.50
3	33.0, -115.9	0.59	34.3, -118.5	1.13
4	37.5, -121.1	0.25	36.9, -121.5	1.01
5	40.3, -124.6	0.31	40.5, -125.2	0.53
6	37.2, -116.2	0.26	37.2, -116.2	0.71
7	33.8, -118.9	0.32	34.2, -117.9	0.61
8	36.3, -121.3	0.17	36.1, -120.5	0.67
Japan				
1	41.5, 141.7	0.54	42.1, 141.7	0.73
2	44.1, 148.6	0.86	44.3, 148.4	0.99
3	34.1, 135.4	0.75	35.3, 133.2	1.48
4	40.3, 142.4	0.67	37.5, 141.6	0.67
5	41.9, 142.4	0.77	40.3, 143.6	0.95
6	37.3, 142.4	0.63	38.5, 141.6	0.64
7	33.9, 135.3	0.72	31.9, 137.4	1.47
8	38.7, 141.8	0.89	41.4, 142.2	0.69
Central Asia				
1	35.6, 49.7	0.96	35.0, 47.6	1.16
2	42.1, 72.6	0.51	40.1, 75.2	1.07
3	30.4, 68.0	0.57	30.0, 68.8	0.72
4	34.1, 59.6	0.65	33.5, 61.0	1.27
5	33.1, 87.0	1.21	35.3, 86.4	0.92
6	39.2, 54.5	0.80	37.6, 56.0	0.90
7	24.4, 68.8	1.08	24.6, 68.6	1.26
8	34.5, 91.7	0.61	34.5, 91.7	0.92
9	36.6, 71.7	0.94	36.5, 71.8	0.83

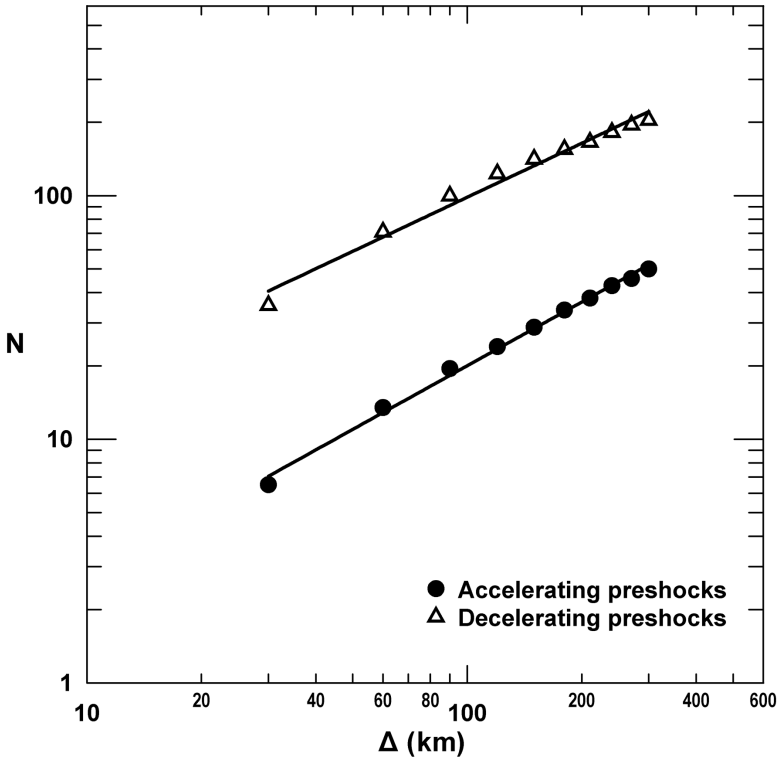

Fig. 2 - Variation of the cumulative frequency, $N(\Delta)$, of the mean number of decelerating preshocks (triangles) and accelerating preshocks (dots) with distance, Δ (in km), from their corresponding physical centers, P_f and P_q.

is more than 0.90 in all cases. The geographical points P_f and P_q are considered as the "physical centers" of the decelerating and accelerating preshocks, respectively.

Another way to determine a representative value of the scaling coefficient D is by stacking the data from all forty-three sequences. In the present work, this was made in the following way. The values of Δ are separated in equal intervals (i.e. 30 km each) and the mean number of shocks of the forty-three sequences in each interval is calculated. Then, the cumulative number, N, of the mean numbers is calculated and log$N$ is linearly correlated with logΔ. Fig. 2 shows the variation of the cumulative frequency, N, of the mean number of accelerating preshocks (dots) with the distance, Δ (in km), from their physical center, P_q, and of decelerating preshocks (triangles) from their physical center, P_f. The linear correlation between log$N$ and logΔ is very high (r>0.99) in both cases. The scaling coefficient D_q=0.87 for accelerating preshocks and D_f=0.74 for decelerating preshocks is in good agreement with the mean values resulting from the correlation of log$N$ with logΔ for each one accelerating and decelerating preshock sequence, respectively.

Fig. 3 shows the spatial distribution of the D values for the decelerating preshocks (upper part) and accelerating preshocks (lower part) of the most recent, largest mainshock examined (M=8.3) that occurred in Japan on 25.9.2003 (number 5 of the mainshocks occurred in Japan in Table 1. The star in this figure corresponds to the epicenter of the mainshock, while dots denote

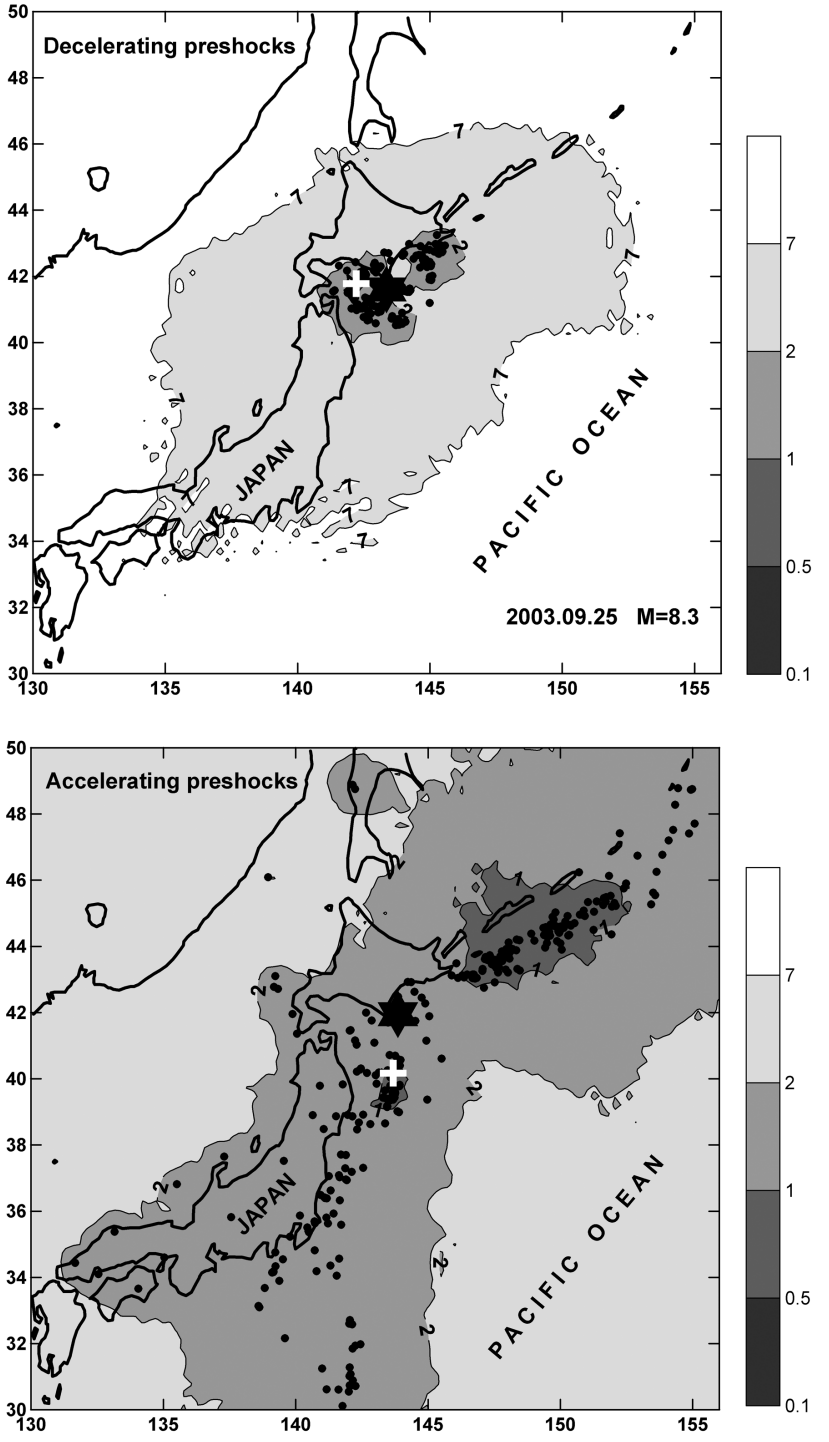

Fig. 3 - Space distribution of D_f values (upper part) for decelerating preshocks and D_q values (lower part) for accelerating preshocks of the big earthquake that occurred in Japan on 25.9.2003 (number 5 on Table 1 for the mainshocks occurring in Japan). The star shows the epicenter of the mainshock and the dots the epicenters of preshocks. The lowest D values in both maps are denoted by crosses. The scales on the right-hand side of the figure show the values of D. The darker shaded parts correspond to values of D smaller than 1 and 2 in the lower and upper parts of the figure, respectively.

the epicenters of preshocks. The grid points that correspond to the lowest exponent values D_f and D_q are also shown (crosses). We can observe that low exponent values ($D_f \leq 2.0$) for decelerating preshocks are concentrated within a relatively small area around the epicenter of the mainshock, by contrast to the size of the area where similar values ($D_q \leq 2.0$) for accelerating preshocks have been calculated. These calculations have been made for 13,000 grid points in both maps. Fig. 4 shows the variation of the cumulative frequency, N, of the accelerating (dots) and decelerating (triangles) preshocks that preceded the Japan 2003 earthquake, with the distance, Δ (in km), from their respective physical centers, P_q and P_f, marked by crosses in Fig. 3.

5. Contribution to the location of mainshocks

The geometrical center, F, of the seismogenic region and the geometrical center, Q, of the critical region are related to the generation of the mainshock. The same holds for the physical center, P_f, of the seismogenic region and the physical center, P_q, of the critical region defined in the present work. It is, therefore, reasonable to assume that these four geographical points (F, P_f, Q, P_q), which are known before the generation of the mainshock, have some relation to the mainshock epicenter, E, of the ensuing mainshock. Thus, these known four points can be used to estimate (predict) the mainshock epicenter of the corresponding ensuing mainshock.

Papazachos *et al*. (2006a) have already based themselves on F and Q to propose an effective procedure for locating the mainshock epicenter by considering the mean distances of these two geometrical centers from the mainshock epicenters of mainshocks that have already occurred. This procedure can be improved by using also the mean distances of P_f and P_q from the epicenters of mainshocks that have already occurred.

From information given on Table 2, it appears that the mean distances from the epicenter, E, and the corresponding standard deviation of the four centers (F, P_f, Q, P_q) are:

$$(EF) = 120 \pm 50 \text{ km}, (EP_f) = 120 \pm 80 \text{ km}, (EQ) = 220 \pm 90 \text{ km}, (EP_q) = 140 \pm 70 \text{ km}. \quad (6)$$

A simple and effective way of using Eq. (6) for the estimation (prediction) of each of the geographical coordinates (latitude, longitude) of the mainshock is to consider it as the weighted average of the corresponding geographical coordinates of the four known points with weights proportional to the inverse of the sum of the mean distance and one standard deviation (1/170, 1/200, 1/310, 1/210). That is, the weights are 0.31 for F, 0.27 for P_f, 0.17 for Q and 0.25 for P_q. A retrospective application of this procedure shows a location of the epicenter of the ensuing mainshock with uncertainty ≤ 150 km, with high probability.

6. Discussion

We have shown that the distances of the epicenters of preshocks (generalised foreshocks) for each one of the preshock sequences considered in the present work from the mainshock epicenter also follow a power-law relation [Eq. (5)] with a constant $D<2$ ($d<0$). The average value of D for both decelerating and accelerating preshock sequences (distances measured from the mainshock epicenter) is almost equal to unit (D_f=0.98±0.45, D_a=1.03±0.30). Therefore, a fractal spatial

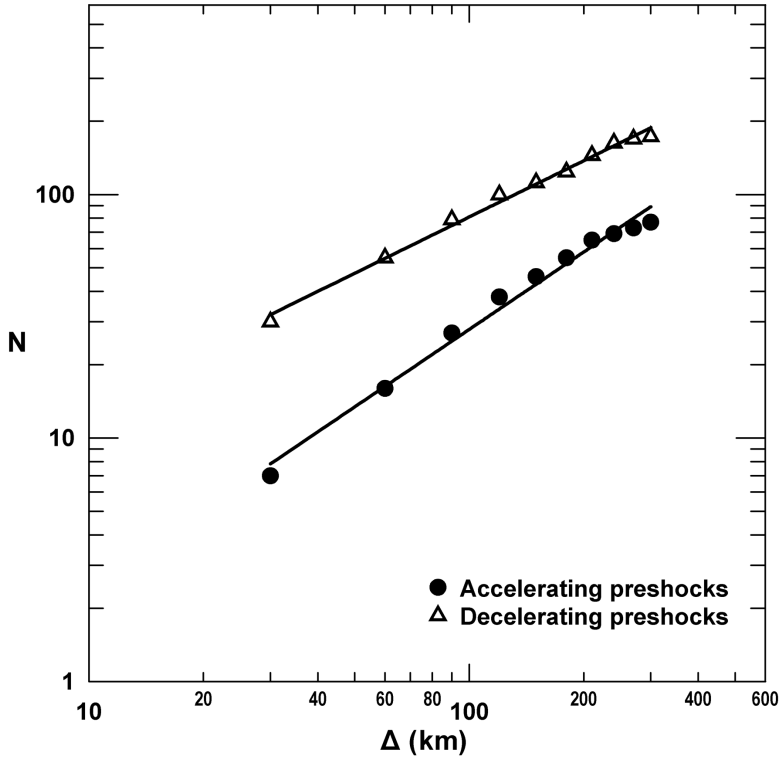

Fig. 4 - Variation of the cumulative frequency, N, of the number of accelerating (dots) and decelerating (triangles) preshocks that preceded the Japan 2003 earthquake, with distance, Δ (in km), from their respective physical centers, P_q and P_f, which are denoted by crosses in Fig. 3.

distribution of preshocks from the mainshock epicenter with a D constant, practically equal to a unit, is observed for both the decelerating and accelerating preshock sequences. This observation suggests that the generation of a decelerating and of the corresponding accelerating preshock sequence is physically related to the generation of the coming mainshock, hence, the predictive properties of these preshock sequences have a physical base.

In addition to the critical earthquake model, other models have also been proposed to explain precursory accelerating seismicity. Such a recently proposed model is the Stress Accumulation Model (Bowman and King, 2001; King and Bowman, 2003; Mignan *et al*., 2006), based on the estimation of the space distribution of the pre-mainshock static stress due to creep at depth and slip on adjacent faults. This model interprets satisfactorily, properties of decelerating preshocks because it predicts regions (lobes) of stress decrease (shadow lobes), that extend to such distances from the mainshock focus where a decelerating strain is observed. This model also predicts a decrease of the shadow area, with time, to the mainshock, in agreement with an observed, similar decrease of seismic deceleration (Papazachos *et al*., 2007).

We should point out that as precursory events with predictive properties we have considered only the preshocks that follow the power-law Eq. (1) in the time domain (with $m>1$ for decelerating preshocks and $m<1$ for accelerating preshocks) as well as additional constraints

concerning the duration of the preshock sequences and the size of the region where these preshocks are located (Papazachos *et al*., 2006a). Furthermore, it has been shown in the present work that the frequency (number of earthquakes per unit area) of these preshocks also fulfils the power-law Eq. (5) in the space domain. Therefore, the results presented in this work suggest an additional constraint followed by the preshock data, which can be also used for intermediate-term prediction of strong mainshocks.

The investigation of plots similar to those presented in Fig. 3 for all mainshocks listed in Table 1, indicated that low D_f values calculated for decelerating preshocks are confined to relatively small areas close to the mainshock epicentre, whereas similar values calculated for accelerating preshocks, (D_q), occupy much broader areas. Moreover, in some cases we observed that more than one cluster of low D_q values located at some distance from the mainshock epicenter may exist. This is the reason why the area with the geographical center as centre of the seismogenic region is examined to define both physical centers.

Papazachos *et al*. (2006a) performed random tests for the occurrence of accelerating and decelerating sequences in such catalogues. They concluded that the probability of the simultaneous occurrence of an accelerating and a decelerating preshock sequence before a mainshock due to the catalogue randomness is small (~10%). We can, therefore, make the reasonable assumption that the probability for the validity, in a random catalogue, of Eq. (5) for an accelerating and a decelerating preshock sequence is also small.

Acknowledgements. We would like to thank the Associate Editor Dr. Lawrence J. Hutchings and the two anonymous reviewers for their comments and suggestions which helped us clarify certain issues and improve the original manuscript.

REFERENCES

Allègre C.J. and Le Mouël J.L.; 1994: *Introduction of scaling techniques in brittle failure of rocks.* Phys. Earth Planet. Inter., **87**, 85-93.

Bowman D.D., Quillon, G., Sammis, C.G., Sornette, A. and Sornette D.; 1998: *An observational test of the critical earthquake concept*. J. Geophys. Res., **103**, 24359-24372.

Bowman D.D. and King G.C.; 2001: *Accelerating seismicity and stress accumulation before large earthquakes.* Geophys. Res. Lett., **28**, 4039-4042.

Brehm D.J. and Braile L.W.; 1999: *Intermediate-term earthquake prediction using the modified time-to-failure method in southern California.* Bull. Seism. Soc. Am., **89**, 275-293.

Bufe C.G. and Varnes D.J.; 1993: *Predictive modeling of seismic cycle of the Great San Francisco Bay Region*. J. Geophys. Res., **98**, 9871-9883.

Karakaisis G.F., Scordilis, E.M., Papazachos, C.B. and Papazachos B.C.; 2006: *A catalogue of earthquakes in California for the period 1901-2005.* Publ. Geoph. Laboratory, University of Thessaloniki.

Karakaisis G.F., Scordilis E.M., Papazachos C.B. and Papazachos B.C.; 2007: *Frequency-magnitude variations of accelerating and decelerating preshocks*. Tectonophysics (submitted).

King G.C. and Bowman D.D.; 2003: *The evolution of regional seismicity between large earthquakes.* J. Geophys. Res., **108**, 1-16, (doi:101029/2001JB000783).

Knopoff L., Levshina T., Keilis-Borok V.J. and Mattoni C.; 1996: *Increased long-range intermediate-magnitude earthquake activity prior to strong earthquakes in California.* J. Geophys. Res., **101**, 5779-5796.

Mignan A., Bowman D.D. and King G.C.; 2006: *An observational test of the origin of accelerating moment release before large earthquakes.* J. Geophys. Res., **111**, B11304, (doi:10.1029/2006JB004374).

Mogi K.; 1969: *Some features of the recent seismic activity in and near Japan II. Activity before and after great earthquakes.* Bull. Earthquake Res. Inst., Univ. Tokyo, **47**, 395-417.

Papazachos B.C. and Papazachos C.B.; 2000: *Accelerated preshock deformation of broad regions in the Aegean area.* Pure appl. Geophys., **157**, 1663-1681.

Papazachos C.B., and Papazachos B.C.; 2001: *Precursory accelerating Benioff strain in the Aegean area*. Ann. Geofis., **144**, 461-474.

Papazachos C.B., Karakaisis G.F., Scordilis E.M. and Papazachos B.C.; 2005a: *Global observational properties of the critical earthquake model.* Bull. Seism. Soc. Am., **95**, 1841-1855.

Papazachos C.B., Scordilis E.M., Karakaisis G.F., and Papazachos B.C.; 2005b: *Decelerating preshock seismic deformation in fault regions during critical periods.* Bull. Geol. Soc. Greece, **36**, 1490-1498.

Papazachos C.B., Karakaisis G.F., Scordilis E.M., and Papazachos B.C.; 2006a: *New observational information on the precursory accelerating and decelerating strain energy release.* Tectonophysics, **423**, 83-96.

Papazachos B.C., Comninakis P.E., Scordilis E.M., Karakaisis G.F, and Papazachos C.B.; 2006b: *A catalogue of earthquakes in Mediterranean and surrounding area for the period 1901-2005.* Publ. Geoph. Laboratory, University of Thessaloniki.

Papazachos C.B., Karakaisis G.F., Papazachos B.C., Scordilis E.M., Panagiotopoulos D.G. and Papaioannou Ch.A.; 2007: *Predictive properties of the decelerating-accelerating seismic strain model*. Publication of Geophysical Laboratory, Univ. of Thessaloniki, **679**, 1-30.

Robinson R.; 2000: *A test of the precursory accelerating moment release model on some recent New Zealand earthquakes*. Geophys. J. Int., **140**, 568-576.

Rundle J.B., Klein W., Turcotte D.L. and Malamud B.D.; 2000: *Precursory seismic activation and critical point phenomena.* Pure Appl. Geophys., **157**, 2165-2182.

Rundle J.B., Turcotte D.L., Shcherbakov R., Klein W. and Sammis C.; 2003: *Statistical physics approach to understanding the multiscale dynamics of earthquake fault systems.* Rev. Geophys., **41**, 1019-1048.

Scordilis E.M., Karakaisis G.F., Papazachos C.B., and Papazachos B.C.; 2006a: *A catalogue of earthquakes in Japan for the period 1901-2005.* Publ. Geoph. Laboratory, University of Thessaloniki.

Scordilis E.M., Papazachos C.B., Karakaisis G.F. and Papazachos B.C.; 2006b: *A catalogue of earthquakes in central Asia for the period 1901-2005.* Publ. Geoph. Laboratory, University of Thessaloniki.

Sornette A. and Sornette D.; 1990: *Earthquake rupture as a critical point. Consequences for telluric precursors*. Tectonophysic, **179**, 327-334.

Sornette D. and Sammis C.G.; 1995: *Complex critical exponents from renormalization group theory of earthquakes: implications for earthquake predictions.* J. Phys. I. **5**, 607-619.

Sykes L.R. and Jaumé S.; 1990: *Seismic activity on neighbouring faults as a long term precursor to large earthquakes in the San Francisco Bay area.* Nature, **348**, 595-599.

Tocher D.; 1959: *Seismic history of the San Francisco bay region*. Calif. Div. Mines Spec. Rep., **57**, 39-48.

Tzanis A., Vallianatos F. and Makropoulos K.; 2000: *Seismic and electrical precursors to the 17-1-1983, M=7 Kefallinia earthquake, Greece, signatures of a SOC system*. Phys. Chem. Earth, **25**, 281-287.

Corresponding author: George F. Karakaisis
Dept. of Geophysics, Aristotle Univ. of Thessaloniki
54124 Greece
phone: +2310 99 8484; fax: +2310 99 8528; e-mail: karakais@geo.auth.gr